ANTIOXIDANTS & REDOX SIGNALING
Volume 14, Number 11, 2011

DOI: 10.1089/ars.2010.3552

ORIGINAL RESEARCH COMMUNICATION

Sulfiredoxin Protects Mice from Lipopolysaccharide-Induced Endotoxic Shock

Anne-Gaëlle Planson,[1] Gaël Palais,[1] Kahina Abbas,[2] Matthieu Gerard,[3] Linhdavanh Couvelard,[4] Agnès Delaunay,[1] Sylvain Baulande,[4] Jean-Claude Drapier,[2] and Michel B. Toledano[1]

Abstract

Peroxiredoxins constitute a major family of cysteine-based peroxide-scavenging enzymes. They carry an intriguing redox switch by undergoing substrate-mediated inactivation *via* overoxidation of their catalytic cysteine to the sulfinic acid form that is reverted by reduction catalyzed by the sulfinic acid reductase sulfiredoxin (Srx). The biological significance of such inactivation is not understood, nor is the function of Srx1. To address this question, we generated a mouse line with a null deletion of the Srx1-encoding *Srxn1* gene. We show here that $Srxn1^{-/-}$ mice are perfectly viable and do not suffer from any apparent defects under laboratory conditions, but have an abnormal response to lipopolysaccharide that manifests by increased mortality during endotoxic shock. Microarray-based mRNA profiles show that although the response of $Srxn1^{-/-}$ mice to lipopolysaccharide is typical, spanning all spectrum and all pathways of innate immunity, it is delayed by several hours and remains intense when the response of $Srxn1^{+/+}$ mice has already dissipated. These data indicate that Srx1 activity protects mice from the lethality of endotoxic shock, adding this enzyme to other host factors, as NRF2 and peroxiredoxin 2, which by regulating cellular reactive oxygen species levels act as important modifiers in the pathogenesis of sepsis. *Antioxid. Redox Signal.* 14, 2071–2080.

Introduction

Peroxiredoxins (Prxs) constitute a major family of cysteine-based peroxide-scavenging enzymes conserved throughout evolution (18, 32). In mammals, Prxs consist of six related members (Prx1 to Prx6) that differ by the number of cysteine (Cys) residues used for catalysis and by their subcellular localization. In typical 2-Cys Prxs (Prx1 to Prx4), peroxide is reduced by the so-called peroxidatic Cys (Cys_P) of one subunit that oxidizes to a sulfenic acid (–SOH) intermediate (43). The –SOH then condensates with the resolving Cys residue of the other subunit to a disulfide, which is reduced by thioredoxin and NADPH, thereby completing the cycle. Based on enzymatic characteristics and high *in vivo* protein abundance, Prxs are thought to be efficient scavengers of very low concentrations of H_2O_2 (18), which agree well with the unique ability of these enzymes to prevent the chromosome instability resulting from the low levels cellular endogenous peroxide production in both yeast (21, 31) and mammals (16), and with the tumor prone phenotype of Prx1 knockout mice (28). Prxs also scavenge peroxinitrite and have been involved in the regulation of H_2O_2 signaling through modalities that are not completely understood (18, 32, 35).

Typical 2-Cys Prxs carry an intriguing redox switch, undergoing peroxide-mediated inactivation *via* overoxidation of Cys_P to the sulfinic acid ($R\text{-}SO_2H$) form (11, 41, 42) that is reverted by a slow ATP-dependent enzymatic process catalyzed by the sulfinic acid reductase sulfiredoxin (Srx) (4, 10). Inactivation only occurs during enzymatic cycling and is proportional to the amount of substrate at both non-saturating and saturating conditions. The biological significance of Prx reversible inactivation is not understood. The observation that inactivation is an attribute of eukaryotic but not prokaryotic enzymes has led to suggest that it is an acquired gain of function selected for regulatory purposes (42). Only typical 2-Cys Prx are overoxidation sensitive because they carry an additional helix absent in overoxidation-insensitive enzymes, which slows down the rate at which Cys_P–SOH condensates with Cys residue, allowing its further oxidation by H_2O_2 (42). It has thus been proposed that Prx inactivation could act as a "floodgate" that restricts scavenging to the low levels of endogenously produced H_2O_2, but allows higher levels of H_2O_2

[1]CEA, DSV, IBITECS Laboratoire Stress Oxydants et Cancer, Gif-sur-Yvette, France.
[2]Institut de Chimie des Substances Naturelles, Gif Research Center, FRC 3115, CNRS, Gif-sur-Yvette, France.
[3]CEA, DSV, IBITECS, Epigenetic Regulation and Cancer Team, Gif-sur-Yvette, France.
[4]PartnerChip, Genopole Campus 2, Evry, France.

to signal (42). In *S. pombe*, the Prx enzyme Tpx1 is the H_2O_2 receptor that activates the H_2O_2-stress response regulator Pap1 by catalyzing its oxidation, and its reversible overoxidation constitutes the mechanism that inhibits Pap1 activation when H_2O_2 levels are high (6, 37). In mammals, however, despite many observations of the involvement of Prxs in H_2O_2 signaling, the existence of a Prx H_2O_2 floodgate has never been validated, and no data of a biological utility of Prx inactivation has yet been provided.

Srx appears to be the only known protein capable of catalyzing sulfinic acid reduction; in mammals, Sestrins were also reported to have such activity (9), but a re-examination of their enzymatic properties did not confirm this finding (38). Srx sulfinic reductase activity is dedicated to overoxidized 2-Cys Prxs, and is not known to use any other substrate (39). In yeast, plants, and mammals, a unique gene encodes Srx.

In an effort to understand why are 2-Cys Prx enzymes reversibly inactivated by overoxidation by their substrate, and to gain knowledge of the *in vivo* functions of mammalian Srx, we generated a mouse line with a null deletion of the Srx-encoding *Srxn1* gene. We report here the description of this knockout mouse line. We show that, surprisingly, loss of Srx does not produce any overt phenotype under laboratory growth conditions. Reactive oxygen species (ROS) are thought to have crucial effects during sepsis by both regulating immune cell activation and contributing to tissue injury (1, 22, 26, 36). Further, mice lacking Prx2 (44), Prx3 (25), or the oxidative stress response-regulator NRF2 (34) share the phenotype of a decreased tolerance to sepsis. As Prxs sulfinylation and its reactivation by Srx1 might become important for either mitigating peroxide stress and/or regulating peroxide signaling, we explored the tolerance of *srxn1*$^{-/-}$ mice to lipopolysaccharide (LPS)-induced endotoxic shock. We show that loss of Srx causes an abnormal response to LPS, amplifying the innate immune response and decreasing the tolerance to endotoxic shock. Srx1 thus adds to Prx2, Prx3, and NRF2 as host factors that by regulating cellular ROS levels act as important modifiers in the pathogenesis of sepsis.

Materials and Methods

Generation of Srx$^{-/-}$ *mice*

A 3.7 kb fragment 5′ to exon 2 of the *Sxrn1* gene locus was polymerase chain reaction (PCR)-amplified from mouse genomic DNA and cloned between the *Nhe*1 and *Eco*R1 sites of PSJ4. Downstream to this fragment, a PCR-amplified 3.4 kb genomic fragment 3′ to exon 2 was inserted between the *Not*1 and *Xho*1 sites. A 2.1 kb fragment containing a Neomycin-resistance cassette (Neo) was then subcloned at the *Not*1 site of PSJ4 to generate the targeting vector (Fig. 1A). The vector was introduced into AT-1 mouse embryonic stem (ES) cells (a derivative of 129Sv) (a gift from M. Vernet) (8) by electroporation, and G-418-resistant recombinants containing the mutated allele in one of the Srxn1 loci were identified by Southern blot and PCR (Fig. 1A). ES recombinant clones were injected into blastocysts embryos of C57BL/6 mice to produce chimeric mice, which were subsequently bred with C57BL/6 mice to produce F1 Srxn1$^{+/-}$ heterozygotes. These F1 mice were either mated with each other to produce F2 *Srxn1*$^{-/-}$ homozygote mice or were further backcrossed with C57BL/6. One *Srxn1*$^{-/-}$ mouse line was established after both four and seven backcrosses. DNA genotyping was performed on mouse-tail biopsies by Southern blot using a 949 kb *Nhe*I to *Hin*dIII probe spanning Srxn1 exon 1 (Fig. 1A, B), and by reverse transcription-PCR using primers P1, P2, P3, and P4 (Fig. 1A, C). All mice were fed with standard mouse chow and houses in a pathogen-free facility. Animal procedures complied with the guidelines of the French ethics committee for animal research.

Cell cultures

Mouse embryo fibroblast cultures were established by harvesting embryos at embryonic day 13. Head and liver were removed. The remaining embryonic tissue was torn with scissors in phosphate-buffered saline (PBS) containing trypsin (GIBCO–Invitrogen), and incubated 5 min at 37°C. The cells in the supernatant were plated in Dulbecco's modified Eagle's medium + 10% fetal calf serum (FCS), 1% glutamine, 1% penicillin and streptomycin (GIBCO–Invitrogen), and cultured at 37°C in 5% CO_2. Cultures were passed 1:3 after reaching confluence and frozen in liquid nitrogen in DMSO + 10% FCS. Cultures were discarded after reaching passage 7. Mouse bone morrow-derived macrophages (BMDMs) were established as described (13), and grown in RPMI + 10% FCS, 2 m*M* glutamine, and 10% L-929-derived conditioned medium.

Monitoring ROS levels by fluorescence

Mouse BMDMs that were left untreated or were incubated during 3 h with *N*-acetylcysteine (10 m*M*) or during 30 min with H_2O_2 (100 μM) were washed with Ca^{2+}- and Mg^{2+}-free PBS, detached using trypsin-EDTA, washed again, and suspended in PBS containing 5-(and-6)-chloromethyl-2′,7′-dichlorodihydrofluorescein diacetate, acetyl ester (CM-H2DCFDA; 10 m*M*; Molecular Probes, Invitrogen), and incubated at 37°C for 30 min. ROS levels were indirectly measured by CM-H2DCFDA fluorescence emission on a Beckman Coulter Cytomics FC500 flow cytometer.

Western blot analyses

Cells were washed on ice with PBS, and lysed in RIPA buffer (Tris-HCl pH 8 [50 M*m*], NaCl [300 m*M*], triton X-100 [1%], and EDTA 1 m*M*). Centrifuged, cleared lysates were diluted with 1/3 final volume of 3× loading buffer (Tris-HCl pH 6.8 [0.2 *M*], glycerol [45%], SDS [6%], β-mercaptoethanol [6% v/v], and bromophenol blue [0.03%]). After heat-denaturation, proteins were separated by SDS-PAGE, transferred onto a nitrocellulose membrane, and immuno-stained in blocking buffer ODYSSEY (Li-Cor Biosciences) with polyclonal rabbit antibodies specific for Srx (1/2000) (10), the SO_2H/SO_3H forms of mammalian 2-Cys Prxs (40) (gifts from Dr. S. G. Rhee), or GAPDH (1/10000; AMBION). Membranes were stripped with the NewBlot Nitro Stripping buffer (Li-Cor Biosciences) when needed. Detection was performed after chromophore-coupled secondary-antibody staining, using the LI-COR Odyssey infrared imager.

Treatments

Endotoxic shock was induced by intraperitoneal (IP) injection of LPS (*Escherichia coli*, serotype 0111:B4, lot number 028K4090; Sigma) at a dosage of 10–100 μg/g of body weight in wild-type and *srxn1*$^{-/-}$ mice that were matched for age (10–16 weeks) and gender. PBS (20 μl/g) was injected in

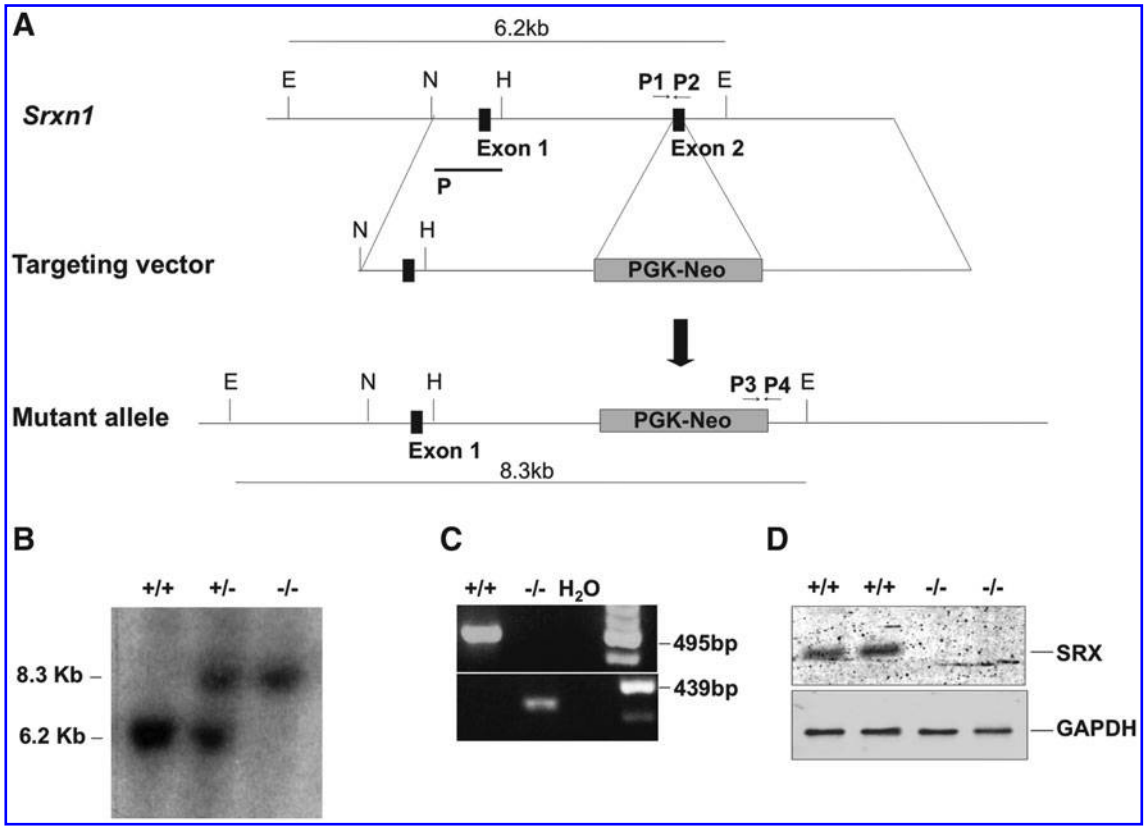

FIG. 1. Generation of *Srxn1*$^{-/-}$ mice. (A) Schematic representation of the mouse *Srxn1* gene, the targeting construct, and the resulting mutant allele. The recognition sites for *Eco*RV (E), *Nhe*I (N), and *Hin*dIII (H) restriction enzymes are indicated. Exons encoding *Srx1* are represented by black boxes. *Dashed lines* indicate the regions of homology used for homologous recombination. *Solid lines* indicate fragment sizes detected by probe P following *Eco*RV digest of genomic DNA. P1 and P2, and P3 and P4 indicate PCR primers used for genotyping the *Srxn1* wild-type and mutant alleles, respectively. **(B)** Southern blot of mouse-tail biopsies showing bands of 6.2 and 8.3 kb that indicate the presence of the wild-type and mutant alleles, respectively. **(C)** PCR genotyping of mouse-tail biopsies using P1 and P2 or P3 and P4 primers and showing a band of 495 bp present in the wild-type allele and absent in the mutant and a band of 439 bp present in the mutant and absent in the wild-type. **(D)** Western blot analysis of Srx1 expression in the liver of wild-type and *Srxn1*$^{-/-}$ mice. GAPDH serves as loading control. PCR, polymerase chain reaction; Srx, sulfiredoxin.

control animals. Survival was monitored by inspection every 4 h for 5 days. Data were expressed as means ± standard error of the mean. Blood was withdrawn from the orbital sinus of anesthetized animals and collected in tubes containing EDTA (2 mg/ml blood) and serum collected after centrifugation. Alanine aminotransferase (ALT), aspartate aminotransferase (AST), creatinine, creatine kinase, glucose, albumin, bilirubin, lactate dehydrogenase, lactate, and alkaline phosphatase were measured on an Olympus AU400 (CEFI, Institut Claude Bernard). Blood analyses (white blood cells and red blood cell counts, hematocrit, hemoglobin, erythrocyte indexes—Mean Corpuscular Hemoglobin, Mean Corpuscular Hemoglobin Concentration, Mean Corpuscular Volume—, platelets) were performed at the Mouse Clinical Institute.

Histological analyses

Skin, mammary glands, heart, aorta, trachea, lungs, pleura, bone marrow, spleen, thymus, mesenteric lymph nodes, esophagus, stomach, small and large intestines, salivary glands, liver, pancreas, kidney, urinary bladder, ovaries, testis, muscle, brain, and eyes were collected from euthanized mice and processed for routine macroscopic and microscopic histological analysis to detect and analyze systematically organ defects and tissue alterations in mice. Organs were fixed in formalin or Bouin's fluid (testis) and decalcified (bones, whole head). A sample of each organ was embedded in paraffin, sectioned at 5 μm, and stained with hematoxylin and eosin. Analyses were performed at the Mouse Clinical Institute (ICS).

RNA sample preparation for microarray analyses

Groups of three male wild-type or *srxn1*$^{-/-}$ mice matched for age (12 weeks old) were used. Mice were subjected to a nonlethal IP injection of LPS at dosage of 12 μg/g of body weight or of PBS (20 μl/g) (control animals). Lung and spleen were isolated 6 and 20 h after LPS challenge, and 6 h after PBS injection. Total RNA was extracted using the RNeasy Mini kit (Qiagen), according to the manufacturer's recommendations. RNA sample quality was evaluated by capillary electrophoresis using the Agilent RNA 6000 Nano Chip kit, and its concentration measured by its absorbance at 260 nm on a NanoDrop 1000 spectrophotometer. To generate cRNAs, 2 μg of RNA was used to generate first-strand cDNAs using a T7-oligo(DT) primer and Superscript II Reverse Transcriptase

(Affymetrix). Second-strand synthesis used DNA ligase and DNA polymerase I, Rnase H, and then T4 DNA polymerase. Double-stranded cDNA was cleaned up using the GeneChip Sample Cleanup Module (Affymetrix). *In vitro* transcription was carried out using T7 RNA polymerase and a biotinylated nucleotide analogue/ribonucleotide mix for cRNA amplification and biotin labeling (GeneChip IVT Labeling Kit). Biotinylated cRNAs were cleaned up using the GeneChip Sample Cleanup Module, quantified, and fragmented into a mean size of 35–200 nucleotides by incubation at 94°C for 35 min in fragmentation buffer (Affymetrix).

mRNA profiling

mRNA profiling was performed on 12 groups of 3 replicates each (36 samples): PBS control, 6 h after injection, in wild-type and *srxn1*$^{-/-}$ mice, spleens and lungs (12); LPS, 6 h after injection, in wild-type and *srxn1*$^{-/-}$, spleen and lungs (12); LPS, 20 h, in wild-type and *srxn1*$^{-/-}$, spleen and lungs (12). It used GeneChip mouse genome 430 2.0 arrays (Affymetrix) that cover ~34,000 well-characterized mouse genes. Fragmented cRNA were hybridized onto arrays for 16 h at 45°C together with internal hybridization controls (bioB, bioC, bioD, cre, and oligonucleotide B2). Washing and staining procedures were performed in the Affymetrix Fluidics Station 450. Probe arrays were exposed to 10 washes in nonstringent wash buffer A (6× SSPE, 0.01% Tween20) at 30°C, followed by 6 washes in stringent buffer B (100 m*M* MES, 0.1 *M* [Na+], and 0.01% Tween20) at 50°C. Biotinylated cRNA were stained with a streptavidin–phycoerythrin conjugate (SAPE, 10 μg/ml) and washed again 10 times with buffer A. An amplification step was performed using goat IgG (100 μg/ml), and then biotinylated with antistreptavidin antibody (3 μg/ml), each followed by an additional SAPE staining (5 min at 35°C). Arrays were then washed 15 times in buffer A at 35°C before scanning using the Affymetrix GeneChip Scanner 3000. Probe-level expression data (CEL files) were finally produced using the GeneChip® Operating Software (GCOS). Quality-control and statistical analyses (background adjustment, normalization, and probe-level summarization of data) used the GC-Robust Multi-Array average algorithm (GC-RMA) and the statistical packages tool Bioconductor (www.bioconductor.org). Probe sets with significantly differential expression were identified by subjecting the data to unpaired *t*-test and filtered by both fold change and *p*-value. Global transcriptional profiles were observed by 3-dimentional Principal Component Analysis diagrams. Distribution of probe sets according to *p*-value and fold change was represented using volcano plots (not shown). Selected probe sets were then analyzed by the hierarchical clustering method using Cluster and TreeView softwares (17). Functional annotations were performed using EASE/DAVID annotation tools (http://david.abcc.ncifcrf.gov/) and the Kyoto Encyclopedia of Genes and Genomes resource (www.genome.jp/kegg/). Microarray data have been deposited in the EBI Microarray repository ArrayExpress (www.ebi.ac.uk/microarray-as/ae/): E-MEXP-2856.

Results

Generation of Srxn1$^{-/-}$ *mice*

In an effort to understand the physiological function of Srx, we generated a null allele of *Srxn1* in AT-1 ES cells by replacing exon 2 that contains the Srx catalytic domain, with a neomycin-resistance (Neo) gene cassette (Fig. 1A). Recombinant ES cells were injected into blastocysts embryos of C57BL/6 mice to produce chimeric mice, from which were derived *Srxn1*$^{-/-}$ mice. Srx1 inactivation was established by genotypic analysis (Fig. 1A–C) and confirmed by Western blot analysis, which indicated the absence of Srx (Fig. 1C). Srx inactivation was also confirmed by the accumulation of overoxidized Prxs in H_2O_2-treated *Srxn1*$^{-/-}$ but not *Srxn1*$^{+/+}$ mouse embryonic fibroblasts (MEFs), the biochemical signature of defective sulfinic acid reductase activity (Fig. 2A, B). A Western blot with an antibody specific for the sulfinylated form of the four 2-Cys Prxs (I–IV) revealed four bands in untreated MEF lysates of both genotypes, which based on size correspond to Prx1/Prx2 for the two lower ones, to Prx3 for the upper third one, and to Prx4 for the uppermost band. Exposure to H_2O_2 (100 μM) led to an increase in the Prx1/Prx2 SO_2H signal in both *Srxn1*$^{+/+}$ and *Srxn1*$^{-/-}$ MEFs. This signal then declined back to basal levels 6 h after H_2O_2 exposure in *Srxn1*$^{+/+}$ but not in *Srxn1*$^{-/-}$ MEFs, where it remained elevated up to 24 h (Fig. 2A). Compared to wild-type MEFs, Prx1/Prx2 sulfinylation was also much more intense in *Srxn1*$^{-/-}$ MEFs incubated with increasing doses of H_2O_2 (50–500 μM). These data thus not only confirm that Srx1 is inactive in *Srxn1*$^{-/-}$ MEFs, but also indicate that there is no other enzyme that can substitute for Srx1 in reducing sulfinylated Prxs.

Srxn1$^{-/-}$ *mice do not have any spontaneous phenotype*

Homozygous *Srxn1*$^{-/-}$ mice were obtained at the expected wild-type:heterozygote:null frequency. They were fertile and healthy, did not display any spontaneous apparent defects, and had a normal life expectancy. The blood cell count (leukocytes, lymphocytes, platelets, and hematocrit) of 35-week-old *Srxn1*$^{-/-}$ mice (males and females, $n = 10$) was not different from that of age-matched *Srxn1*$^{+/+}$ mice (not shown). A necropsy performed at 34–35 weeks of age ($n = 3$) did not reveal any macroscopic lesions, and a systematic microscopic analysis of these mice (see Materials and Methods) did not reveal either any abnormality that could distinguish *Srxn1*$^{-/-}$ and *Srxn1*$^{+/+}$ mice. The pattern of *Srxn1* tissue expression, established by real-time quantitative PCR, did not reveal either any hint to a physiological role of Srx1 except for a moderately higher expression in the brain (Supplementary Fig. S1; Supplementary Data are available online at www.liebertonline.com/ars). Nevertheless, BMDMs from *Srxn1*$^{-/-}$ mice were abnormal, having significantly higher ROS levels than those of their wild-type counterpart, as shown by the fluorescence of dichlorodihydrofluorescein diacetate (CM-H2DCFDA) (Fig. 2C). The constitutively high ROS levels of *Srxn1*$^{-/-}$ BMDMs decreased upon incubation with the antioxidant compound *N*-acetylcysteine, which suggested that they could result from defective scavenging. Further, exposure to H_2O_2 raised intracellular ROS in wild-type BMDMs to the high levels present in untreated *Srxn1*$^{-/-}$ BMDMs, but not in the latter cells, as if the ROS levels were already maximal in these mutant cells (Fig. 2B). Transcriptomic profiles also showed subtle abnormalities in mutant mice. They were comparatively established in the lungs and spleen of 12-week-old *Srxn1*$^{+/+}$ ($n = 3$) and *Srxn1*$^{-/-}$

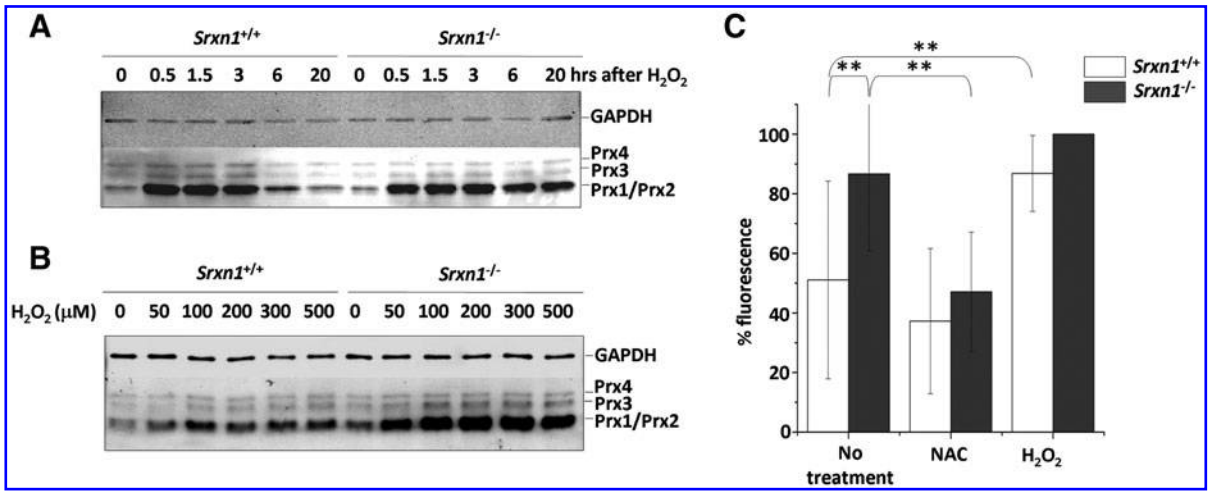

FIG. 2. Srx1 inactivation leads to accumulation of sulfinylated Prx1/Prx2 and increased reactive oxygen species levels. **(A, B)** Mouse embryonic fibroblasts from *Srxn1*$^{+/+}$ and *Srxn1*$^{-/-}$ mice, as indicated, were incubated in the presence of 100 μM H_2O_2 for the indicated time **(A)**, or with the indicate amount of H_2O_2 **(B)** for 3 h, lysed, and analyzed by Western blot sequentially immunostained with antibodies specific for the SO_2/SO_3H form of 2-Cys Prxs, or for GAPDH, as indicated. **(C)** Mouse bone marrow-derived mouse macrophages left untreated or incubated with *N*-acetylcysteine (10 m*M*) for 3 h, or with H_2O_2 (100 μM) for 30 min, were suspended in phosphate-buffered saline containing 5-(and-6)-chloromethyl-2′,7′-dichlorodihydrofluorescein diacetate, acetyl ester and fluorescence emission was measured. Results are mean of three independent experiments. **Significant differences ($p < 0.1$) by the two-tailed Student's *t*-test. NAC, *N*-acetylcysteine; Prx, peroxiredoxin.

($n = 3$) males that had received an IP injection of PBS (see also below); 3248 and 736 differentially expressed transcripts were thus identified in the spleen and lung, respectively. These genes belonged to a very large number of pathways, but, of note, many of those found upregulated in *Srxn1*$^{-/-}$ animals were linked to adaptative and innate immunity, especially in spleen (Supplementary Table S1), which possibly hinted to a silent immune defect.

Mice lacking Srx are highly susceptible to LPS-induced endotoxic shock

The absence of any apparent phenotype in *Srxn1*$^{-/-}$ mice led us to explore experimental conditions that would unravel a phenotype. Prxs sulfinylation is known to occur as a result of Prx enzymatic cycling and of increased peroxide levels and inactivates Prx peroxidase function (18). As Srx1 enzymatic function is to reactivate Prxs by reduction of its sulfinated form, the enzyme could become important for mitigating peroxide stress and/or regulating peroxide signaling. Sepsis provided a good model, as involving the release of ROS by activated phagocytic cells (27), which have microbicidal functions (5), contribute to pathogenesis by causing cellular and tissue damage (1, 36), and amplifies signaling events (22, 29). We used bacterial endotoxin (LPS) administered to mice by IP injection, which replicates the clinical spectrum of septic choc (3), and monitored survival during 5 days. In initial dose–response studies, we established that the dose of 25-to 50 μg/g body weight resulted in the death of 50%–100% of wild-type animals. LPS (25 μg/g) was administered to 3-month-old *Srxn1*$^{+/+}$ ($n = 8$) and *Srxn1*$^{-/-}$ ($n = 8$) male mice (Fig. 3A). Such dose of LPS was lethal for both groups of animals. However, in the *Srxn1*$^{-/-}$ group 100% of the animals had died within the first 24 h after LPS injection, whereas 87.5% of wild-type animals remained alive up to 40 h ($p < 0.001$). To check whether this phenotype crossed genders, we monitored the effect of LPS (25 μg/g) in 3-month-old *Srxn1*$^{+/+}$ ($n = 7$) and *Srxn1*$^{-/-}$ ($n = 5$) female mice (Fig. 3B). As previously observed, C57BL/6 female mice were significantly more resistant to the lethal effect of LPS than males, and this difference was also observed for *Srxn1*$^{-/-}$ mice. Still, *Srxn1*$^{-/-}$ mice were significantly more sensitive to the lethal effect of LPS, as they all died within 3 days, whereas only two *Srxn1*$^{+/+}$ mice died within this period, the remaining five mice being still alive and healthy after 5 days ($p < 0.001$).

Serum levels of the liver damage markers ALT and AST were measured in 5-month-old *Srxn1*$^{+/+}$ ($n = 6$) and *Srxn1*$^{-/-}$ ($n = 6$) males that had received an IP injection of a sublethal dose of LPS (10 μg/g) (Table 1). ALT levels remained low in animals of both genotypes at 6 h but then increased in *Srxn1*$^{-/-}$ mice, but not in *Srxn1*$^{+/+}$. AST levels were similarly moderately augmented at 6 h in mice of both genotypes, but then significantly increased at 24 h in *Srxn1*$^{-/-}$ mice but not *Srxn1*$^{+/+}$ ($p < 0.05$). No significant difference was observed in the serum levels of creatine kinase, lactate dehydrogenase, lactate, alkaline phosphatase, and creatinine (not shown).

These results show that Srx1 clearly protects mice from sterile endotoxic shock.

The genomic response to LPS is delayed in Srxn1$^{-/-}$ *mice*

We searched for transcriptional changes that could explain the differential tolerance of *Srxn1*$^{+/+}$ and *Srxn1*$^{-/-}$ mice to LPS-induced endotoxemia by comparing the spleen and lung mRNA profiles of 12-week-old *Srxn1*$^{+/+}$ ($n = 3$) and *Srxn1*$^{-/-}$ ($n = 3$) males, 6 and 20 h after a nonlethal IP LPS injection (12 μg/g), with those of the same organs from matched animals, 6 h after an IP injection of PBS (see above). Principal Component Analysis (PCA) showed tight triplicate samples

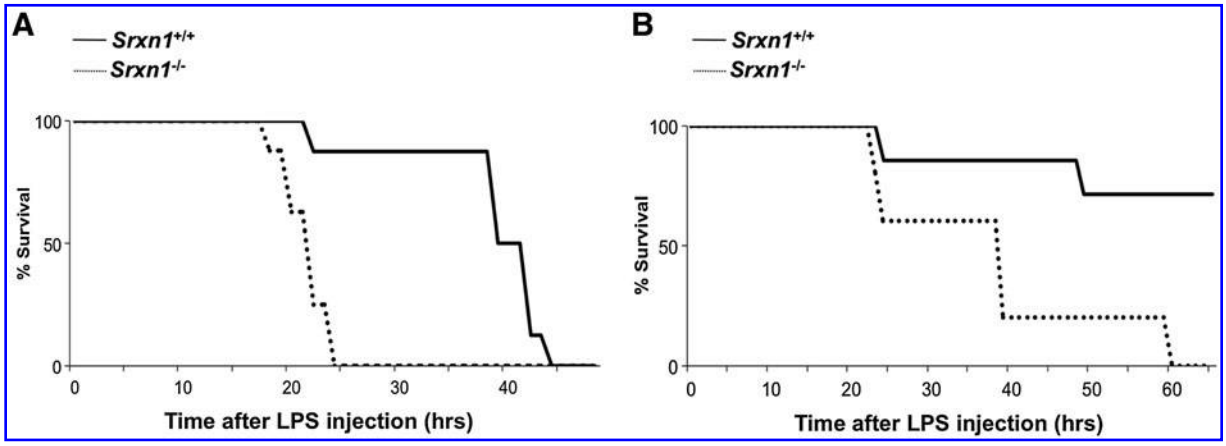

FIG. 3. Increased mortality from LPS-induced endotoxemia in *Srxn1*$^{-/-}$ mice. Survival of 3-month-old males *Srx*$^{+/+}$ ($n=8$) and *Srx*$^{-/-}$ ($n=8$) **(A)** and females *Srxn1*$^{+/+}$ ($n=7$) and *Srxn1*$^{-/-}$ ($n=5$) **(B)** that received an IP injection of LPS (25 μg/g body weight). Viability was recorded every 4 h. *Srxn1*$^{+/+}$ mice had a significant improved survival compared with *srxn1*$^{-/-}$ by the two-tailed Student's *t*-test ($p<0.001$). IP, intraperitoneal; LPS, lipopolysaccharide.

clustering, indicating good reproducibility, and clear divergence between conditions (PBS:6H *vs.* LPS:6H *vs.* LPS:20H), which reflected the extent of the LPS genomic response (Supplementary Fig. S2).

At the 6 h time-point (LPS:6H), wild-type and *Srxn1*$^{-/-}$ mice had both typical responses to LPS that spanned all innate immunity—cytokines, chemokines and their receptors, chemokine signaling, Toll-like, NOD-like, and RIG-I-like receptor and cytosolic DNA-sensing pathways, JAK-STAT signaling, and complement and coagulation cascades—and several adaptive immunity pathways—antigen processing/presentation, NK, and T-cell and B-cell signaling pathways (Supplementary Table S2). However, despite the similarity of the responses of *Srxn1*$^{-/-}$ and *Srxn1*$^{+/+}$ mice, important differences were seen, not so in the number of genes in each of these functional categories (Supplementary Tables S2 and S3), but in the amplitude of gene expression (Fig. 4, Supplementary Fig. S3, and Supplementary Table S4). Messenger RNA level fold changes were significantly higher for many innate immunity-related transcripts in *Srxn1*$^{+/+}$ mice, even upon taking into account the constitutive upregulation of several of these genes in the spleen of *Srxn1*$^{-/-}$ animals. Especially striking was the higher expression in *Srxn1*$^{+/+}$ mice of genes encoding cytokines, chemokines, and costimulatory cell surface molecules (Fig. 4, Supplementary Fig. S3, and Supplementary Table S4), which are crucial effectors of the systemic inflammatory response triggered by LPS. At the 20 h time-point, however, the genomic response was now much more intense in the *Srxn1*$^{-/-}$ mice, with regard to both the number of regulated genes (Fig. 5 and Supplementary Tables S5 and S6) and their expression change (Fig. 4, Supplementary Fig. S3, and Supplementary Table S4). The number of regulated genes indeed substantially decreased in *Srxn1*$^{+/+}$ animals, especially in spleen, whereas it increased in *Srxn1*$^{-/-}$ mice (Supplementary Table S5). Figure 5 depicts the number of regulated genes in the gene clusters the most representative of innate immunity, indicating that at the 6 h time-point they are comparable between genotypes in spleen, whereas at the 20 h time-point they remain high or further increase in both organs of *Srxn1*$^{-/-}$ mice, while they significantly decrease in *Srxn1*$^{+/+}$ mice, especially in spleen (Fig. 5A). Similarly, in lungs the amplitude of gene expression remained high in *Srxn1*$^{-/-}$ mice for many innate immunity genes, whereas it decreased in *Srxn1*$^{+/+}$ mice (Fig. 5B). Especially demonstrative of such trend was exhibited by the fold changes of genes encoding cytokines, chemokines, and costimulatory molecules, which were high at 6 h in *Srxn1*$^{+/+}$ and low in *Srxn1*$^{-/-}$, as mentioned above, but then decreased in the former at 20 h, and increased in the latter, in both spleen (Fig. 4 and Supplementary Table S4) and lungs (Supplementary Fig. S3 and Supplementary Table S4).

Table 1. Alanine Aminotransferase and Aspartate Aminotransferase Serum Levels in Lipopolysaccaride-Challenged Mice

	Alanine aminotransferase	*Aspartate aminotransferase*
Srxn1$^{+/+}$ LPS:6H	19 ± 6	150 ± 42
Srxn1$^{-/-}$ LPS:6H	14 ± 6	140 ± 27
Srxn1$^{+/+}$ LPS:20H	19 ± 4	170 ± 27
Srxn1$^{-/-}$ LPS:20H	241 ± 128	1210 ± 445

Serums were collected 6 and 24 h after LPS injection (10 μg/g body weight), and alanine aminotransferase and aspartate aminotransferase measured (U/L). Data (mean $\pm$ SE) are from 5-month-old *Srxn1*$^{+/+}$ and *Srxn1*$^{-/-}$ male mice ($n=6$) ($p<0.05$).
LPS, lipopolysaccharide.

Discussion

We report here the generation of a mouse line with a null mutation in the gene encoding Srx1, and its description. *Srxn1*$^{-/-}$ mice were fully viable and did not suffer from any apparent clinical and histological defects under laboratory conditions. *Srxn1*$^{-/-}$-derived MEFs were totally defective in reducing the sulfinylated form of Prx1 and Prx2 generated by H_2O_2, which confirmed the Srx1 defect of *Srxn1*$^{-/-}$ mice, and also indicated that no other mouse enzyme can substitute for Srx1 in its Prx-specific sulfinic reductase function. Despite lack of apparent defects, microarray-based mRNA profile

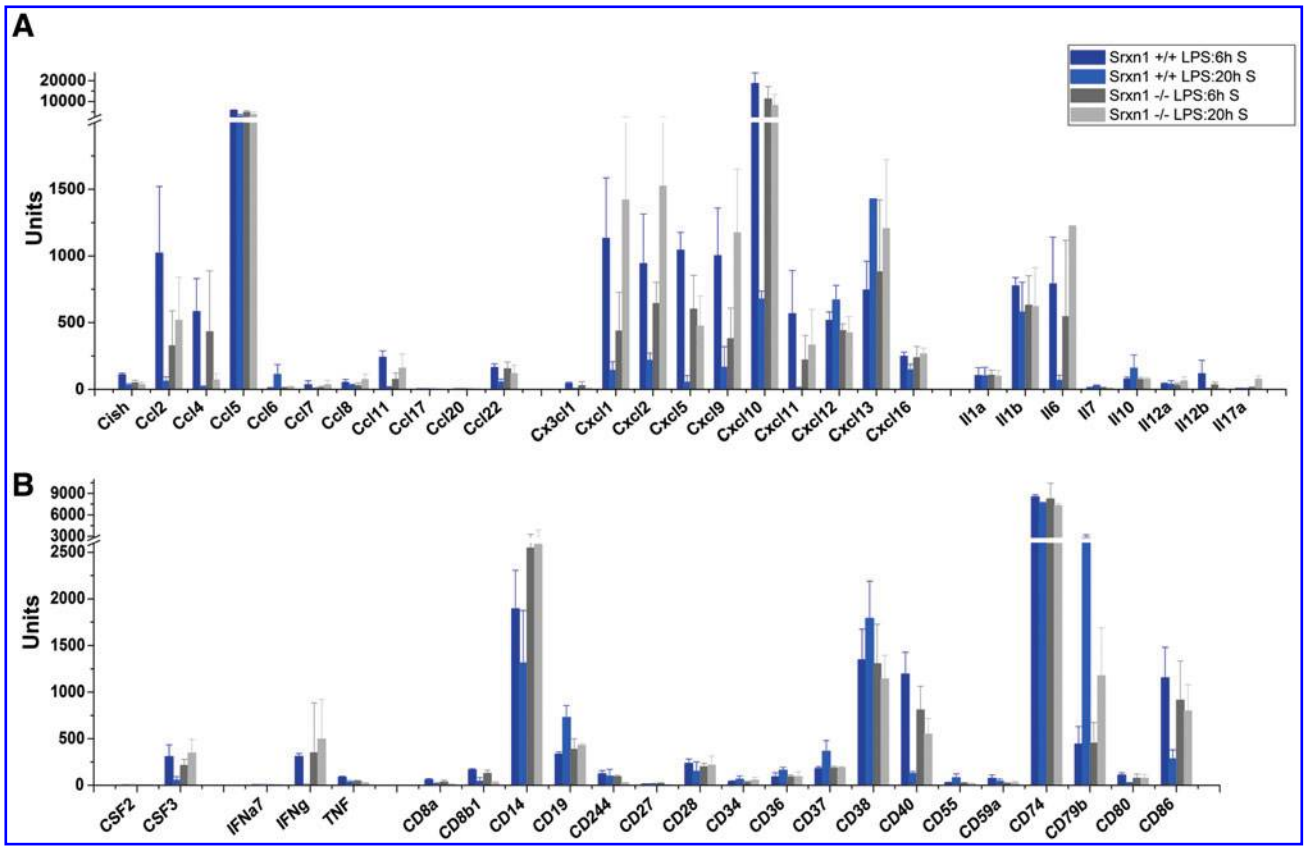

FIG. 4. ***Srxn1*$^{-/-}$ mice have a delayed and prolonged genomic response to LPS.** Absolute mRNA levels of cytokines, chemokines, and interleukins genes **(A)** and of colony-stimulating factors (CSF2 and CSF3), IFNα7 (IFNa7), γ-IFN (IFNg), and TNFα (TNF) **(B)**, in the spleen of *Srxn1*$^{+/+}$ and *Srxn1*$^{-/-}$ 6 and 20 h after IP injection of a sublethal dose of LPS (12 μg/g), as indicated in the figure. Error bars are represented; scale break is between 2000 and 2500 units in **(A)** and 2600 and 2800 units **(B)**. Data are from the same microarray as in Figure 5. (To see this illustration in color the reader is referred to the web version of this article at www.liebertonline.com/ars).

analysis showed that *Srxn1*$^{-/-}$ mice upregulated several genes linked to adaptive and innate immunity under laboratory conditions, which possibly indicates a silent immune defect. Further, compared to their wild-type counterpart, they had an abnormal response to LPS that manifested by a significantly increased mortality during endotoxic shock, and a delayed and prolonged genomic response to LPS. Microarray-based mRNA profiles showed that the response of *Srxn1*$^{-/-}$ mice to LPS was in fact typical, in terms of the nature of the genes regulated, which spanned the all spec-

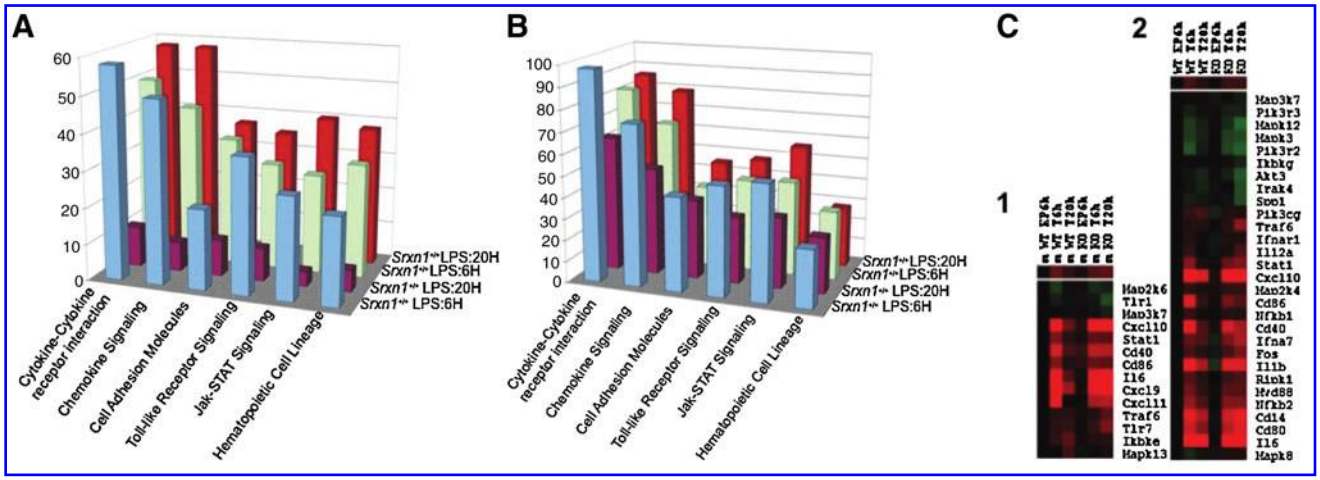

FIG. 5. Srx1 acts as a physiological negative regulator of LPS signaling. Number of regulated genes in Kyoto Encyclopedia of Genes and Genomes functional clusters in spleen **(A)** and lungs **(B)** of *Srxn1*$^{+/+}$ and *Srxn1*$^{-/-}$ mice 6 and 20 h after an IP injection of a subtoxic dose of LPS (12 μg/g), as indicated. **(C)** Minimum and maximum expression fold differences of representative differentially expressed genes in *Srxn1*$^{-/-}$ *versus* *Srxn1*$^{+/+}$ displayed as a heat map after a log2 transformation and gene-level normalization using expression values of phosphate-buffered saline–treated *Srxn1*$^{+/+}$mice. The *red color* indicates upregulated genes, and the *green color*, downregulated ones. All data are from the same microarrays as in Figure 4. (To see this illustration in color the reader is referred to the web version of this article at www.liebertonline.com/ars).

trum of pathways triggered during activation of innate immunity as well as several pathways of adaptive immunity. However, compared to *Srxn1*$^{+/+}$ mice, this response was delayed by several hours, and remained intense or even increased at late time after LPS injection (20 h), when the response of *Srxn1*$^{+/+}$ mice had already largely dissipated. Such prolonged response was particularly marked with regard to the proinflammatory cytokines IL1β and IL6, which are essential effectors of the inflammatory response (12, 14), and for several chemokines, including Ccl2, Ccl11, Ccl20, Ccl22, Cx3cl1, Cxcl1, Cxcl2, Cxcl5, Cxcl9, Cxcl10, and Cxcl11, that have essential functions in leukocyte chemotaxis at sites of inflammation and injury (24). Such prolonged response was observed for many other genes of immunity as γ-IFN that stimulates inducible nitric oxide synthase-dependent nitric oxide production by macrophages and cell surface MHC molecules expression, the macrophage cell surface costimulatory molecules CD14 that amplifies LPS responsiveness of Toll-like receptor 4 (TLR4), CD40 that activates macrophage upon binding CD154 on activated T cells, and CD86 that activates T cells by binding CD28 receptor, and also for genes encoding innate immunity kinases and transcription factors (Supplementary Fig. S4). Such a delayed and prolonged genomic response to LPS is consistent with the poor clinical tolerance of *Srxn1*$^{-/-}$ animals to endotoxic shock, which clearly indicates that Srx activity protects mice from the lethality of endotoxic shock.

What is the basis for the role of Srx during endotoxemia, and how it relates to its enzymatic function? The function of Srx is to reactivate 2-Cys Prxs when in their sulfinylated inactive form. Prxs themselves constitute an important protection against cellular damage caused by peroxide and peroxinitrite, and have also demonstrated functions in H_2O_2 signaling (7, 18, 35). LPS-induced systemic inflammation is initiated by LPS binding to TLR4 on the surface of monocytic cells, and TLR4-proximal and distal signaling critically involve ROS produced by membrane NADPH oxidase (26). Prx2 was recently shown to exert a negative control on LPS-TLR4 signaling by holding check on the levels of ROS produced by NADPH oxidases (44), which corroborate the fact that mice lacking Prx2, as those lacking Srx1 (this study), are hypersensitive to the lethality of LPS-induced endotoxemia (44). Srx may therefore influence sepsis by controlling the strength of TLR4 signaling through its effect on Prx2. Disruption of NRF2, a transcription factor that controls the cellular redox poise by regulating antioxidants, including Prxs, activities of the thioredoxin and glutathione pathways, and phase II enzymes (15, 20), also amplifies LPS-TLR4 signaling and causes a drastic increase in lethality during LPS-induced endotoxic shock (34), an effect that is dependent on the NADPH oxidase catalytic subunit gp91^{phox} (23). Interestingly, NRF2 regulates not only the expression of Prxs (13) but also that of Srx1 (2, 19, 30, 33). Further, we have recently shown that in LPS/γ-IFN-stimulated mouse macrophages, inducible nitric oxide synthase-derived NO activates NRF2-dependent Srx expression (Abbas *et al.*, manuscript submitted). *Nrf2*$^{-/-}$-derived macrophages were in fact unable to reduce over-oxidized Prx1/Prx2, indicating that in these cells Srx expression is strictly dependent upon NRF2. We also showed in this study that NO treatment increases peroxide scavenging and decrease peroxide levels in wild-type-derived but not *Srxn1*$^{-/-}$-derived macrophages, thus linking LPS-induced macrophage NO production and the induction of an important NRF2-Srx antioxidant pathway. This study (Abbas *et al.*, manuscript submitted), together with the data of Thimmulappa (34) and Kong (23) and the data presented here, thus suggests that the abnormal LPS response of mice lacking Srx or NRF2 might be caused by the defective NO-dependent induction of the NRF2-Srx antioxidant axis that exacerbates TLR4 signaling and the ensuing systemic inflammatory response by loss of control on the levels of NADPH oxidase-produced ROS. Prx2 might also be part of this antioxidant axis, but it is not induced by NO (13). The NRF2-Srx antioxidant axis could, however, also be important for protecting macrophages, and possibly other cells, from NADPH oxidase-produced ROS damage. However, the abnormal regulation of many genes of adaptive and innate immunity in untreated *Srxn1*$^{-/-}$ mice, and the peculiar delayed and prolonged LPS response of these mice both suggest a defect in a regulatory rather than in an oxidative damage protective mechanism. Whereas loss of Prx, or NRF2, or as shown here Srx decreases the tolerance to LPS-induced endotoxemia, the loss of catalase increases this tolerance (45), which has led these authors to suggest that H_2O_2 could have anti-inflammatory effects by inhibiting the proteasome, and hence NF-κB activation. Such opposite roles of antioxidants during sepsis might, nevertheless, be reconciled by considering that Prxs (and Srx) are only active under very low levels of H_2O_2, whereas catalase becomes an efficient antioxidant at much higher H_2O_2 levels (18). Accordingly during sepsis, the deficiency in Prx or Srx should amplify H_2O_2 signaling, which presumably proceeds at low levels H_2O_2, whereas the deficiency in catalase should favor a buildup of H_2O_2 levels, high enough to prevent NF-κB activation.

In conclusion, the present study further indicates that Srx adds to Prx2, Prx3, and NRF2 as host factors that by regulating cellular ROS levels act as important modifiers in the pathogenesis of sepsis.

Acknowledgments

We greatly acknowledge Patrick Hery for his expert help with mice experiments; Drs. Benoît Biteau, Flora Tomasello, and Agniezska Sekowska for their help in the initial stage of the *Srxn1*$^{-/-}$ mouse line generation; and Dr. Sue Goe Rhee for his kind gift of reagents. This work was supported by grants from Association pour la Recherche Centre le Cancer (ARC) and Agence Nationale de la Recherche (ANR) SOLEMA to M.B.T., and ANR NOPEROX to J.-C.D. and M.B.T. A.-G.P. was supported by an ANR fellowship NOPEROX. M.B.T. is the recipient of a fund program, "Equipe Labellisée Ligue 2009," from La Ligue Contre le Cancer.

Author Disclosure Statement

There are no competing financial interests with regard to the data included in this article for any of its authors.

References

1. Babior BM. Phagocytes and oxidative stress. *Am J Med* 109: 33–44, 2000.
2. Bae SH, Woo HA, Sung SH, Lee HE, Lee SK, Kil IS, and Rhee SG. Induction of sulfiredoxin via an Nrf2-dependent path-

way and hyperoxidation of peroxiredoxin III in the lungs of mice exposed to hyperoxia. *Antioxid Redox Signal* 11: 937–948, 2009.
3. Beutler B. Inferences, questions and possibilities in Toll-like receptor signalling. *Nature* 430: 257–263, 2004.
4. Biteau B, Labarre J, and Toledano MB. ATP-dependent reduction of cysteine-sulphinic acid by S. cerevisiae sulphiredoxin. *Nature* 425: 980–984, 2003.
5. Bogdan C, Rollinghoff M, and Diefenbach A. Reactive oxygen and reactive nitrogen intermediates in innate and specific immunity. *Curr Opin Immunol* 12: 64–76, 2000.
6. Bozonet SM, Findlay VJ, Day AM, Cameron J, Veal EA, and Morgan BA. Oxidation of a eukaryotic 2-Cys peroxiredoxin is a molecular switch controlling the transcriptional response to increasing levels of hydrogen peroxide. *J Biol Chem* 280: 23319–23327, 2005.
7. Bryk R, Griffin P, and Nathan C. Peroxynitrite reductase activity of bacterial peroxiredoxins. *Nature* 407: 211–215, 2000.
8. Buchou T, Vernet M, Blond O, Jensen HH, Pointu H, Olsen BB, Cochet C, Issinger OG, and Boldyreff B. Disruption of the regulatory beta subunit of protein kinase CK2 in mice leads to a cell-autonomous defect and early embryonic lethality. *Mol Cell Biol* 23: 908–915, 2003.
9. Budanov AV, Sablina AA, Feinstein E, Koonin EV, and Chumakov PM. Regeneration of peroxiredoxins by p53-regulated sestrins, homologs of bacterial AhpD. *Science* 304: 596–600, 2004.
10. Chang TS, Jeong W, Woo HA, Lee SM, Park S, and Rhee SG. Characterization of mammalian sulfiredoxin and its reactivation of hyperoxidized peroxiredoxin through reduction of cysteine sulfinic acid in the active site to cysteine. *J Biol Chem* 279: 50994–51001, 2004.
11. Chevallet M, Wagner E, Luche S, van Dorsselaer A, Leize-Wagner E, and Rabilloud T. Regeneration of peroxiredoxins during recovery after oxidative stress: only some over-oxidized peroxiredoxins can be reduced during recovery after oxidative stress. *J Biol Chem* 278: 37146–37153, 2003.
12. Cohen J. The immunopathogenesis of sepsis. *Nature* 420: 885–891, 2002.
13. Diet A, Abbas K, Bouton C, Guillon B, Tomasello F, Fourquet S, Toledano MB, and Drapier JC. Regulation of peroxiredoxins by nitric oxide in immunostimulated macrophages. *J Biol Chem* 282: 36199–36205, 2007.
14. Dinarello CA. Proinflammatory and anti-inflammatory cytokines as mediators in the pathogenesis of septic shock. *Chest* 112: 321S–329S, 1997.
15. Dinkova-Kostova AT, Holtzclaw WD, and Kensler TW. The role of Keap1 in cellular protective responses. *Chem Res Toxicol* 18: 1779–1791, 2005.
16. Egler RA, Fernandes E, Rothermund K, Sereika S, de Souza-Pinto N, Jaruga P, Dizdaroglu M, and Prochownik EV. Regulation of reactive oxygen species, DNA damage, and c-Myc function by peroxiredoxin 1. *Oncogene* 24: 8038–8050, 2005.
17. Eisen MB, Spellman PT, Brown PO, and Botstein D. Cluster analysis and display of genome-wide expression patterns. *Proc Natl Acad Sci U S A* 95: 14863–14868, 1998.
18. Fourquet S, Huang ME, D'Autreaux B, and Toledano MB. The dual functions of thiol-based peroxidases in H2O2 scavenging and signaling. *Antioxid Redox Signal* 10: 1565–1576, 2008.
19. Glauser DA, Brun T, Gauthier BR, and Schlegel W. Transcriptional response of pancreatic beta cells to metabolic stimulation: large scale identification of immediate-early and secondary response genes. *BMC Mol Biol* 8: 54, 2007.
20. Hayes JD and McMahon M. NRF2 and KEAP1 mutations: permanent activation of an adaptive response in cancer. *Trends Biochem Sci* 34: 176–188, 2009.
21. Huang ME and Kolodner RD. A biological network in Saccharomyces cerevisiae prevents the deleterious effects of endogenous oxidative DNA damage. *Mol Cell* 17: 709–720, 2005.
22. Kolls JK. Oxidative stress in sepsis: a redox redux. *J Clin Invest* 116: 860–863, 2006.
23. Kong X, Thimmulappa R, Kombairaju P, and Biswal S. NADPH oxidase-dependent reactive oxygen species mediate amplified TLR4 signaling and sepsis-induced mortality in Nrf2-deficient mice. *J Immunol* 185: 569–577, 2010.
24. Le Y, Zhou Y, Iribarren P, and Wang J. Chemokines and chemokine receptors: their manifold roles in homeostasis and disease. *Cell Mol Immunol* 1: 95–104, 2004.
25. Li L, Shoji W, Takano H, Nishimura N, Aoki Y, Takahashi R, Goto S, Kaifu T, Takai T, and Obinata M. Increased susceptibility of MER5 (peroxiredoxin III) knockout mice to LPS-induced oxidative stress. *Biochem Biophys Res Commun* 355: 715–721, 2007.
26. Nathan C and Ding A. Nonresolving inflammation. *Cell* 140: 871–882, 2010.
27. Nathan C and Ding A. SnapShot: reactive oxygen intermediates (ROI). *Cell* 140: 951–951.e2, 2010.
28. Neumann CA, Krause DS, Carman CV, Das S, Dubey DP, Abraham JL, Bronson RT, Fujiwara Y, Orkin SH, and Van Etten RA. Essential role for the peroxiredoxin Prdx1 in erythrocyte antioxidant defence and tumour suppression. *Nature* 424: 561–565, 2003.
29. Niethammer P, Grabher C, Look AT, and Mitchison TJ. A tissue-scale gradient of hydrogen peroxide mediates rapid wound detection in zebrafish. *Nature* 459: 996–999, 2009.
30. Papadia S, Soriano FX, Leveille F, Martel MA, Dakin KA, Hansen HH, Kaindl A, Sifringer M, Fowler J, Stefovska V, McKenzie G, Craigon M, Corriveau R, Ghazal P, Horsburgh K, Yankner BA, Wyllie DJ, Ikonomidou C, and Hardingham GE. Synaptic NMDA receptor activity boosts intrinsic antioxidant defenses. *Nat Neurosci* 11: 476–487, 2008.
31. Ragu S, Faye G, Iraqui I, Masurel-Heneman A, Kolodner RD, and Huang ME. Oxygen metabolism and reactive oxygen species cause chromosomal rearrangements and cell death. *Proc Natl Acad Sci U S A* 104: 9747–9752, 2007.
32. Rhee SG, Chae HZ, and Kim K. Peroxiredoxins: a historical overview and speculative preview of novel mechanisms and emerging concepts in cell signaling. *Free Radic Biol Med* 38: 1543–1552, 2005.
33. Singh A, Ling G, Suhasini AN, Zhang P, Yamamoto M, Navas-Acien A, Cosgrove G, Tuder RM, Kensler TW, Watson WH, and Biswal S. Nrf2-dependent sulfiredoxin-1 expression protects against cigarette smoke-induced oxidative stress in lungs. *Free Radic Biol Med* 46: 376–386, 2009.
34. Thimmulappa RK, Lee H, Rangasamy T, Reddy SP, Yamamoto M, Kensler TW, and Biswal S. Nrf2 is a critical regulator of the innate immune response and survival during experimental sepsis. *J Clin Invest* 116: 984–995, 2006.
35. Toledano MB, Planson AG, and Delaunay-Moisan A. Reining in H(2)O(2) for safe signaling. *Cell* 140: 454–456, 2010.
36. Victor VM, Rocha M, and De la Fuente M. Immune cells: free radicals and antioxidants in sepsis. *Int Immunopharmacol* 4: 327–347, 2004.

37. Vivancos AP, Castillo EA, Biteau B, Nicot C, Ayte J, Toledano MB, and Hidalgo E. A cysteine-sulfinic acid in peroxiredoxin regulates H2O2-sensing by the antioxidant Pap1 pathway. *Proc Natl Acad Sci U S A* 102: 8875–8880, 2005.
38. Woo HA, Bae SH, Park S, and Rhee SG. Sestrin 2 is not a reductase for cysteine sulfinic acid of peroxiredoxins. *Antioxid Redox Signal* 11: 739–745, 2009.
39. Woo HA, Jeong W, Chang TS, Park KJ, Park SJ, Yang JS, and Rhee SG. Reduction of cysteine sulfinic acid by sulfiredoxin is specific to 2-cys peroxiredoxins. *J Biol Chem* 280: 3125–3128, 2005.
40. Woo HA, Kang SW, Kim HK, Yang KS, Chae HZ, and Rhee SG. Reversible oxidation of the active site cysteine of peroxiredoxins to cysteine sulfinic acid. Immunoblot detection with antibodies specific for the hyperoxidized cysteine-containing sequence. *J Biol Chem* 278: 47361–47364, 2003.
41. Woo HA, Yim SH, Shin DH, Kang D, Yu DY, and Rhee SG. Inactivation of peroxiredoxin I by phosphorylation allows localized H(2)O(2) accumulation for cell signaling. *Cell* 140: 517–528, 2010.
42. Wood ZA, Poole LB, and Karplus PA. Peroxiredoxin evolution and the regulation of hydrogen peroxide signaling. *Science* 300: 650–653, 2003.
43. Wood ZA, Schroder E, Robin Harris J, and Poole LB. Structure, mechanism and regulation of peroxiredoxins. *Trends Biochem Sci* 28: 32–40, 2003.
44. Yang CS, Lee DS, Song CH, An SJ, Li S, Kim JM, Kim CS, Yoo DG, Jeon BH, Yang HY, Lee TH, Lee ZW, El-Benna J, Yu DY, and Jo EK. Roles of peroxiredoxin II in the regulation of proinflammatory responses to LPS and protection against endotoxin-induced lethal shock. *J Exp Med* 204: 583–594, 2007.
45. Zmijewski JW, Lorne E, Zhao X, Tsuruta Y, Sha Y, Liu G, and Abraham E. Antiinflammatory effects of hydrogen peroxide in neutrophil activation and acute lung injury. *Am J Respir Crit Care Med* 179: 694–704, 2009.

Address correspondence to:
Prof. Michel B. Toledano
Laboratoire Stress Oxydants et Cancer
CEA, DSV, IBITECS
CEA-Saclay Bat 142
91191 Cedex Gif-sur-Yvette
France

E-mail: michel.toledano@cea.fr

Date of first submission to ARS Central, August 9, 2010; date of final revised submission, October 26, 2010; date of acceptance, November 14, 2010.

Abbreviations Used

ALT = alanine aminotransferase
AST = aspartate aminotransferase
BMDM = bone marrow-derived mouse macrophage
CM-H2DCFDA = 5-(and-6)-chloromethyl-2′,7′-dichlorodihydrofluorescein diacetate, acetyl ester
Cys_P = peroxidatic Cys
ES cells = embryonic stem cells
FCS = fetal calf serum
IP = intraperitoneal
KEGG = Kyoto Encyclopedia of Genes and Genomes
LPS = lipopolysaccharide
MEF = mouse embryonic fibroblast
NAC = *N*-acetylcysteine
PBS = phosphate-buffered saline
PCR = polymerase chain reaction
Prx = peroxiredoxin
ROS = reactive oxygen species
Srx = sulfiredoxin
TLR4 = Toll-like receptor 4

This article has been cited by:

1. Robert R. Bowers, Yefim Manevich, Danyelle M. Townsend, Kenneth D. Tew. 2012. Sulfiredoxin Redox-Sensitive Interaction with S100A4 and Non-Muscle Myosin IIA Regulates Cancer Cell Motility. *Biochemistry* **51**:39, 7740-7754. [CrossRef]
2. Fei Yin , Harsh Sancheti , Enrique Cadenas . Mitochondrial Thiols in the Regulation of Cell Death Pathways. *Antioxidants & Redox Signaling*, ahead of print. [Abstract] [Full Text HTML] [Full Text PDF] [Full Text PDF with Links]
3. Diane E. Handy , Joseph Loscalzo . 2012. Redox Regulation of Mitochondrial Function. *Antioxidants & Redox Signaling* **16**:11, 1323-1367. [Abstract] [Full Text HTML] [Full Text PDF] [Full Text PDF with Links]
4. In Sup Kil, Se Kyoung Lee, Keun Woo Ryu, Hyun Ae Woo, Meng-Chun Hu, Soo Han Bae, Sue Goo Rhee. 2012. Feedback Control of Adrenal Steroidogenesis via H2O2-Dependent, Reversible Inactivation of Peroxiredoxin III in Mitochondria. *Molecular Cell* **46**:5, 584-594. [CrossRef]
5. Woojin Jeong, Soo Han Bae, Michel B. Toledano, Sue Goo Rhee. 2012. Role of sulfiredoxin as a regulator of peroxiredoxin function and regulation of its expression. *Free Radical Biology and Medicine* . [CrossRef]
6. Magdalena L. Circu, Tak Yee Aw. 2011. Redox biology of the intestine. *Free Radical Research* 1-22. [CrossRef]
7. Heta Merikallio, Paavo Pääkkö, Vuokko L. Kinnula, Terttu Harju, Ylermi Soini. 2011. Nuclear factor erythroid-derived 2-like 2 (Nrf2) and DJ1 are prognostic factors in lung cancer. *Human Pathology* . [CrossRef]